Bull Volcanol (2001) 63:264–273
DOI 10.1007/s004450100143

RESEARCH ARTICLE

F. Gamberi

Volcanic facies associations in a modern volcaniclastic apron (Lipari and Vulcano offshore, Aeolian Island Arc)

Received: 6 April 2000 / Accepted: 31 March 2001 / Published online: 27 June 2001

Abstract Multibeam bathymetric and reflectivity data, high-resolution sidescan sonar mapping and ROV images have allowed reconstruction of the present-day facies distribution within the volcaniclastic apron offshore from Lipari and Vulcano. Primary volcanic, resedimented volcaniclastic and volcanogenic sedimentary facies have been distinguished. Primary volcanic facies are volumetrically subordinate but play a major role in controlling the distribution of the other facies and the development of the main submarine canyons, and as the source of volcanic detritus in resedimented volcaniclastic facies. Erosion and transport prevail in the canyons. Conversely, deposition of volcanogenic sediments, in response to flow spreading and gradient reduction, occurs at the canyon mouths. The influence of the adjacent islands on the offshore processes is particularly evident in the area facing the active sector of Vulcano Island. Here, large volumes of volcanogenic sediment from the emergent volcanic edifice are transferred downslope by subaqueous gravity flows allowing the construction of a volcaniclastic fan.

Keywords Seafloor reflectivity · Volcaniclastic apron · Primary volcanic facies · Resedimented volcaniclastic facies · Volcanogenic sediment · Aeolian Island Arc · Tyrrhenian Sea

Introduction

Widespread, kilometre-thick volcaniclastic aprons typically represent more than 90% of the rock volume of volcanic island arcs (Orton 1996; Carey 2000). The composition and facies associations of these aprons are governed by the interplay between the island arc volcano-tectonic evolution and the nature of the transporting and depositional processes (Carey 2000). Facies associations within volcaniclastic aprons are basically governed by the interaction between volcanism, producing abundant volcanic debris, and surface processes responsible for erosion, transport and deposition (Fisher and Schmincke 1994). Additional controls over facies associations in volcaniclastic aprons are: the nature and location of subaerial and subaqueous eruptive centres, which influence sediment supply and create and modify topography; volcanotectonism that causes local rapid uplift and subsidence; and steep slopes, frequent earthquakes and hydrothermal alteration of the volcanic pile which favour slope failure events (McPhie et al. 1993). Thus, volcaniclastic aprons typically comprise complex assemblages of primary volcanic, resedimented volcaniclastic and volcanogenic sedimentary facies (McPhie 1995; McPhie et al. 1993).

Current facies models for volcaniclastic aprons are based mainly on observations of uplifted ancient successions, whereas studies of present-day analogues are rare and mainly regional in scope (Orton 1996; Wright 1996).

In this paper we present a detailed study of the present-day volcaniclastic apron extending offshore east of Lipari and Vulcano Islands. The seafloor features of the study region were deciphered using a composite data set consisting of multibeam bathymetry and reflectivity data, sub-bottom profiles, sidescan sonar images and ROV records. These data provide constraints on volcanic and sedimentary processes, allowing reconstruction of the present-day facies distribution, in accordance with the classification proposed by McPhie et al. (1993) and McPhie (1995). The factors which control facies distribution in this modern volcaniclastic apron are also discussed.

Geological setting

Lipari and Vulcano are the southernmost islands of the Aeolian arc, an active volcanic belt developed above the

Editorial responsibility: J. McPhie

F. Gamberi (✉)
Istituto per la Geologia Marina di Bologna,
Via Gobetti 101, 40129 Bologna, Italy
e-mail: fabiano@igm.bo.cnr.it
Fax: +39-546-6398922, Tel.: +39-051-6398922
Fax: +39-051-6398940

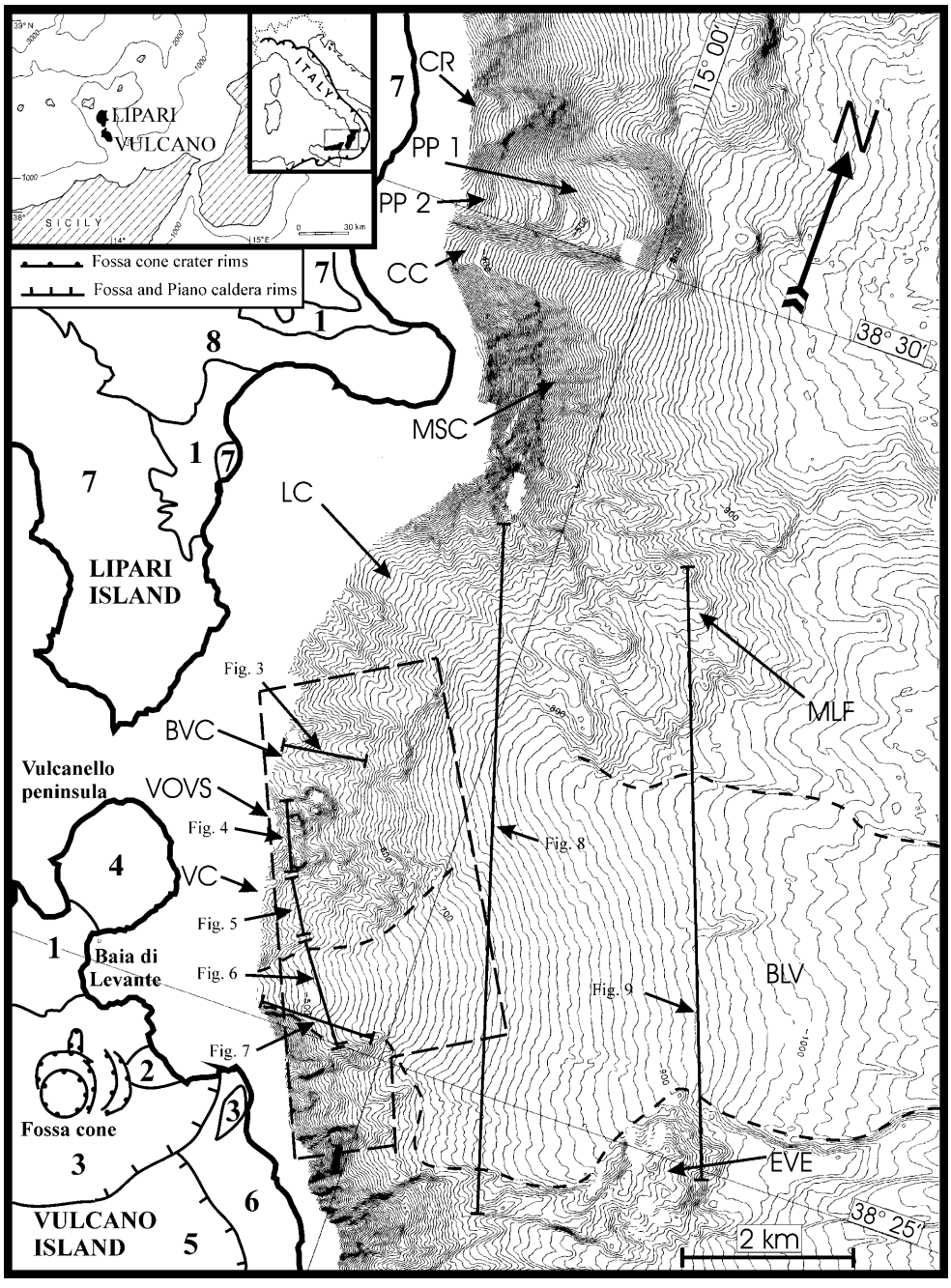

Fig. 1 Location (top left corner inset) and bathymetric map of the study region. *1* Alluvium and beach deposits; *2* area affected by the 1988 landslide; *3* pyroclastic deposits and lavas of La Fossa Cone; *4* Vulcanello lava platform and pyroclastic deposits; *5* Piano Caldera infill; *6* Primordial Vulcano; *7* Lipari island volcanic units of the youngest phases; *8* Lipari island volcanic units of the oldest phase. *CR* Capo Rosso lava; *PP2* Punta Papesca 2 lava; *PP1* Punta Papesca 1 lava; *CC* Canneto canyon; *MSC* Monterosa submarine cone; *LC* Lipari canyon; *MLF* Monterosa lava field; *BVC* Bocche di Vulcano canyon; *VOVS* Vulcanello offshore volcanic seamounts; *VC* Vulcanello canyon; *BLV* Baia di Levante valley; *EVE* eccentric volcanic edifice. The *dashed line* marks the boundary of the Baia di Levante Valley. In the area within the *rectangle*, high-resolution sidescan sonar data are available. *Bold lines* are segments of sidescan sonar and subbottom profiles illustrated in this paper. The land data are from De Astis et al. (1997), Ventura (1994), De Rosa et al. (1985) and Crisci et al. (1991)

northwestward-subducting Ionian plate (Fig. 1, upper left inset; Barberi et al. 1974, 1994). The volcanic islands are constructed on a continental basement at a depth of approximately 1000 m (Fabbri et al. 1981; Gabbianelli et al. 1991).

Lipari Island is made up of volcanic rocks ranging in age from approximately 223 ka to historical time (Pichler 1980; De Rosa et al. 1985; Crisci et al. 1991). The eastern side of the island is composed mainly of products of the youngest volcanic phases: pyroclastic deposits and rhyolite domes dating from 42 to 20 ka in the south, and pyroclastic deposits and lavas emplaced from 17 ka to historical time in the north (Fig. 1). Older products occur only in the Monterosa promontory and consist mainly of pyroclastic sequences erupted from 150 to 127 ka (Fig. 1). Gamberi and Marani (1997) presented a detailed correlation of the volcanic units exposed in the eastern side of Lipari with the offshore morphobathymetric features.

The island of Vulcano is formed by four main volcanic elements: the Primordial Vulcano; the Lentia Complex; La Fossa Cone; and the Vulcanello peninsula (Fig. 1; Ventura 1994; De Astis et al. 1997). In the southeastern sector of Vulcano Island, the composite cone of Primordial Vulcano (120–100 ka) is made up of lavas and minor pyroclastic units (Fig. 1; De Astis et al. 1997).

In the northeastern sector of the island, the Fossa Caldera faces the sea (Fig. 1). It was formed after 15 ka, following the partial destruction of the older Primordial Vulcano and Lentia Complex (24–15 ka), and is filled by pyroclastic deposits and lavas erupted between 15 and 8 ka. In the centre of the Fossa Caldera is La Fossa Cone, an active, 391-m-high, steep-sided volcano (Fig. 1). La Fossa Cone was formed in the past 6 ka by pyroclastic deposits and minor lavas; its last eruption dates back to 1888–1890 (Mercalli and Silvestri 1891; Frazzetta et al. 1983; Ventura 1994; De Astis et al. 1997). Repeated periods of volcanic unrest have followed this eruption; the best known one, culminating in 1987–1990, was characterised by an increase of maximum temperature of the fumaroles, ground deformation and the opening of many new fractures on La Fossa Cone (Barberi et al. 1991). Seismic swarms linked to the internal dynamics of the volcano are also frequent in the area (Falsaperla and Neri 1986; Cardaci et al. 1988). All these processes, enhanced by a reduction of the shear strength of the volcanic pile due to hydrothermal circulation, favour unstable conditions in La Fossa Cone and in the adjacent areas (Rasa' and Villari 1991). The northeastern slope of La Fossa Cone is characterised by areas of extensive mass movement, and the adjacent sea cliffs show rapid retreat induced by gravity acting on the slope (Rasa' and Villari 1991). A recent landslide affected the seaward flank of La Fossa Cone on 20 April 1988 (Rasa' and Villari 1991). The sliding mass, with a volume of approximately 2×10^5 m^3, entered the sea and generated a small tsunami observed in the nearby village of Porto di Levante (Achilli et al. 1998; Tinti et al. 1999). The peninsula of Vulcanello, the northernmost feature of the island, consists of a lava platform and three nested volcanic cones that formed as a new island in 183 B.C.; younger eruptions resulted in connection with Vulcano around 1550 A.D.

Previous studies eastward offshore from Vulcano (Gabbianelli et al. 1991) revealed the absence of a continental platform and the presence of an eccentric cone located 4 km east of Punta Luccia with its summit at 742 m below sea level (EVE in Fig. 1).

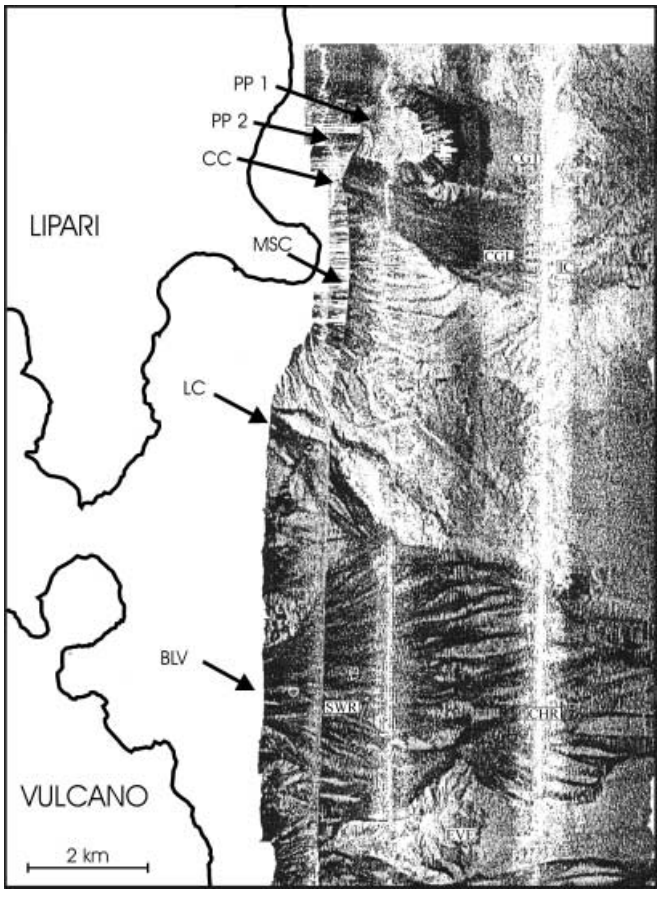

Fig. 2 Multibeam reflectivity data over the study region. Note that reflectivity data do not cover the upper slope portion where bathymetric data are available (see Fig. 1 for comparison). *CGT* coarse-grained talus downslope from the front of the Punta Papesca 1 lava; *CGL* coarse-grained lobe at the mouth of the Canneto canyon; *IC* incised chutes downslope from the CGL; *SWR* swales and ridges on the surface of the Baia di Levante volcaniclastic fan; *CHR* chutes and ridges in the lower BLV. The remaining acronyms and map limits are the same as in Fig. 1

Data set

Bathymetric and reflectivity data acquired with SIMRAD EM1000 and EM12 multibeam systems are available at depths greater than 350 m. A bathymetric map of the study region, obtained with a 25-m grid interval, is shown in Fig. 1; the reflectivity data are shown in Fig. 2.

In addition, "Geoacoustic-Geopulse" sidescan sonar data acquired and processed with an Isis-Triton system were collected at water depths between 300 and 600 m (Fig. 1). High-resolution, 3.5-kHz sub-bottom profiles were collected in parallel with both the multibeam and sidescan sonar lines. Moreover, the volcanic seamounts located offshore from Vulcanello were investigated with a "Super Achilles" ROV, and subsequently sampled (Gamberi et al. 1998).

Lipari offshore

Six submarine lavas have been recognised in the northeastern Lipari offshore area (Gamberi and Marani 1997); three of them are shown in the northern part of Figs. 1 and 2; the remaining three submarine lavas are further north. The morphology of the lavas and their relationships with on-land outcropping units led Gamberi and Marani (1997) to interpret them as the submarine portion of silicic lava flows generated from vents on land.

In the northeastern limit of the reflectivity data (Fig. 2), a high backscatter area marks the rocky surface of the Capo Rosso lava, whereas poor reflectivity data coincide with the Punta Papesca 2 lava. The surface of the silicic Punta Papesca 1 lava is a tongue-shaped, me-

dium backscatter area, up to 1250 m wide, with narrow, concentric high-reflectivity ribbons (Fig. 2). The high reflectivity, downflow-convex ribbons have been interpreted as curved ridges which stand out from the slightly sedimented, medium backscatter lava surface. The spacing of the downflow-convex ridges is approximately 100 m. The high backscatter of the flanks and the front of the lava (Fig. 2) indicates that these steep surfaces are rocky. A high backscatter area that extends downslope from the 200-m-high Punta Papesca 1 lava front (Fig. 2) consists of coarse lava fragments.

A high backscatter area between the Punta Papesca 1 lava and the Monterosa submarine cone marks the floor of the Canneto canyon, with a gradient of 13° and a width of 250 m. The Canneto canyon appears to die out at a depth of approximately 750 m, where a decrease in the slope (9°) is associated with downslope-convex bathymetric contours and high backscatter seafloor (Figs. 1, 2). This seafloor region is lobate in plan (Fig. 2), with a width of approximately 1000 m at a water depth of 950 m and fanning out downslope. We interpret it as a region floored by coarse-grained sediment at the mouth of Canneto canyon (Fig. 2). Further downslope, the seafloor presents medium backscatter, but channelised features in the form of small elongated chutes are present, as is also evident from narrow, high backscatter ribbons (Figs. 1, 2).

The Monterosa submarine cone displays high backscatter, indicating the presence of predominantly coarse-grained detritus, as already suggested by Gamberi and Marani (1997). Conversely, the low backscatter seafloor of the Monterosa lava field (Gamberi and Marani 1997) suggests that it is covered by fine-grained sediments; high backscatter tones, evidence of coarse-grained material, are confined to the depressed areas between the different flow units which constitute the Monterosa lava field.

South of the Monterosa submarine cone, coarse-grained facies flooring the Lipari canyon is represented by high backscatter seafloor. The upper part of Lipari canyon has a width of 500 m and a gradient of 8°. At a depth of approximately 600 m it bifurcates into a southern, 500-m-wide branch and a northern one, 200 m wide. These high backscatter branches diverge downslope on either side of a low backscatter area, which reaches a width of 750 m. Further canyon bifurcation occurs in the wider, southern branch of the Lipari canyon. The various branches of the Lipari canyon connect with the Baia di Levante Valley, a high backscatter area offshore north of Vulcano Island.

Vulcano offshore

In the area between Lipari and the Bocche di Vulcano canyons, the upper slope, down to approximately 700 m, is characterised by alternating ridges and valleys (Fig. 1). High-resolution sidescan sonar images of this portion of the study region show that the ridges and the sides of the valleys are low backscatter areas covered by sediment; rocky outcrops are, however, represented by high backscatter spots (Fig. 3). Other sidescan sonar lines in this area show that gullies and slumps are common on the flanks of the ridges. The floors of the largest valleys, such as the Bocche di Vulcano canyon, are marked by high backscatter tones (Fig. 3). The high backscatter associated with the Bocche di Vulcano canyon dies out at approximately 700 m.

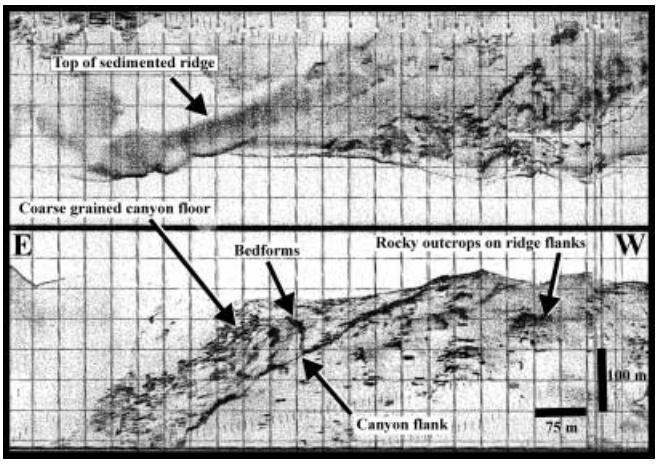

Fig. 3 High-resolution, sidescan sonar image of the Bocche di Vulcano canyon (see Fig. 1 for location). Ship track (*bold line* in the centre of figure) cuts obliquely across the canyon floor. The lower and upper parts of figure show the shallower and deeper portions of the canyon, respectively. A linear, erosional scarp marks the southern flank of the canyon and delimits the high backscatter canyon floor. Note downstream-concave bedforms at the centre of the canyon and the blocky reflective pattern of the northern canyon floor

Adjacent to Vulcanello peninsula, a field of volcanic seamounts is shown by the bathymetric map (Gamberi et al. 1998; Fig. 1). The largest of these seamounts rises 70 m above the surrounding seafloor at a depth of 300 m and is composed of two coalescing cones oriented in a WSW–ENE direction (Fig. 1). The reflective pattern of the seamounts, in the high-resolution sidescan sonar data (Fig. 4) and ROV records, indicate that they are composed mainly of pillow lavas from very recent submarine eruptions, and are covered by only a thin veneer of sediments (Gamberi et al. 1997). Samples collected from one of these volcanic seamounts are basaltic (Gamberi et al. 1998). In addition, ROV images show that in some portions of the seamounts, and particularly at their bases, there are accumulations of pillow fragment breccia composed mostly of large fragments of pillow tubes. A high backscatter reflective pattern characterises the seafloor as far as 1 km downslope from the volcanic cones. The ROV records show that this area is floored by sandy sediment, coarser than the otherwise low backscatter surrounding sediment.

Sediment-covered seafloor extends to the south of the volcanic seamounts. The low-backscatter reflectivity pattern is interrupted by the 200-m-wide floor of the Vulcanello canyon, where narrow, high backscatter features,

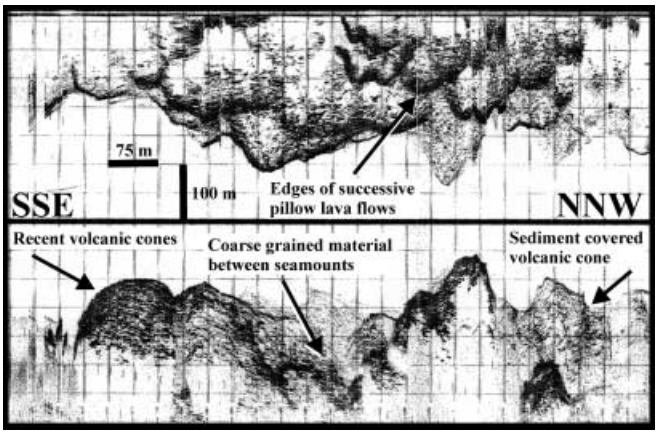

Fig. 4 High-resolution, sidescan sonar image of the Vulcanello offshore volcanic seamounts (location in Fig. 1). Ship track (*bold line* in the centre of figure) is just west of the largest pillow lava cones, imaged in the lower half of figure, offshore from Vulcanello. Note the difference in backscatter tone between the recent cones to the SSE and an older cone, presumably sediment-covered to the NNW. In the upper sidescan sonar swath (upper half of figure), lobate scarps are the edges of successive pillow lavas. Coarse-grained deposits derived from the seamounts accumulate between the pillow lava cones, resulting in high backscatter tones

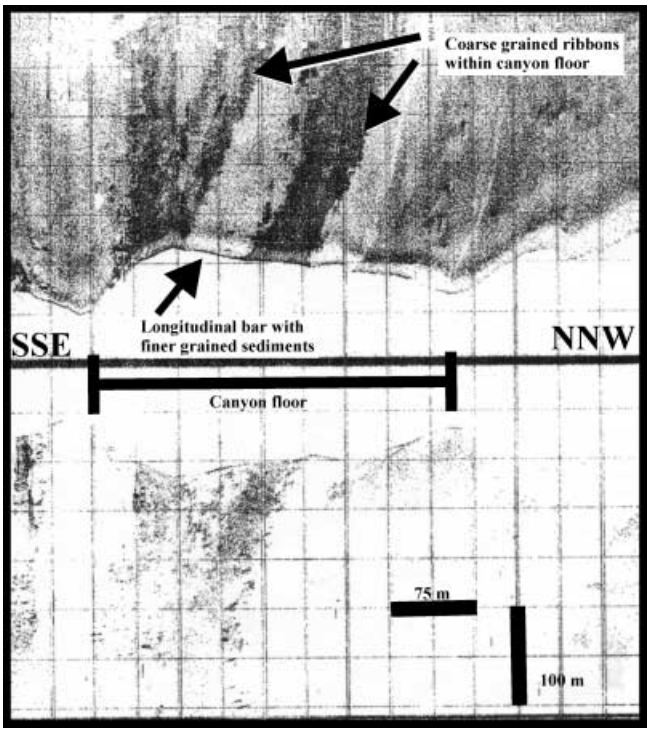

Fig. 5 High-resolution, sidescan sonar image of the Vulcanello canyon (see Fig. 1 for location). Ship track (*bold line* in the centre of figure) crosses the canyon at a depth of approximately 450 m. The upper half of figure shows the canyon floor from a depth of approximately 380 m (top) to approximately 450 m. High backscatter tones correspond to areas covered by coarse-grained deposits, whereas low backscatter characterises a finer-grained longitudinal bar in the central portion of the canyon floor. The geometry of along-slope acquisition accounts for the poorer-quality data over the deeper portions of the canyon in the downslope-looking sidescan sonar swath (lower half of the figure)

elongate in the downstream direction (Fig. 5), variously diverge and converge, isolating low-backscatter elements.

A particular feature of the Vulcano offshore zone is a downslope-widening valley, hereafter named Baia di Levante valley (BLV), facing the Fossa caldera. This valley is characterised by high backscatter tones; however, both across- and along-slope reflectivity texture variations are present. In particular, in a downslope direction, upper, middle and lower portions of the BLV, each characterised by distinctive morphobathymetric and seafloor reflectivity features, can be distinguished.

The upper portion of the BLV, down to approximately 600 m, is characterised by downslope concave bathymetric contours and a gradient of 9° (Fig. 1). Erosional features are well developed at approximately 500 m water depth (Fig. 6) and common on its northern side. In contrast, a pronounced scarp marks the southern boundary of the upper portion of the BLV (Figs. 6, 7). Down to approximately 500 m depth, this scarp is flanked by a high backscatter chute containing dispersed large blocks. The centre of the BLV upper portion is characterised by a homogeneous high backscatter pattern within which, however, some scattered blocks are evident (Fig. 6). These seafloor features suggest that a homogeneous, coarse-grained layer with dispersed large blocks covers the upper portion of the BLV.

The BLV middle portion, down to approximately 800 m, has downslope-concave contours with a gradient of 7°. A sub-bottom profile crossing this portion of the BLV (Fig. 8) indicates that it is the site of a low-relief, coarse-grained fan, with swales of coarse-grained sediment between slightly elevated ridges covered by finer-grained sediment. In the reflectivity map, the swales are downslope-elongated, high-backscatter ribbons running between the low-backscatter ridges. The ridges have maximum length of 1 km and width of 125 m (Fig. 2). The southern and northern margins of the fan are slightly incised by chutes running along the boundary of the BLV (Figs. 1, 8).

The lower portion of the BLV is characterised by a gradient of 4.5° and is bounded by two prominent E/W-trending scarps, which reach a height of 120 m (Figs. 1, 9). From a depth of 800–950 m, the southern boundary scarp follows a NE-elongated ridge coinciding with the eccentric volcanic edifice described by Gabbianelli et al. (1991). This ridge is characterised by a low-backscatter seafloor (Fig. 2), with a 15-m-thick cover of fine-grained sediments, observed in the sub-bottom profiles (Fig. 9). The surface of the lower portion of the BLV is characterised by diamond-shaped low-reflectivity areas isolated within anastomosing high-backscatter areas (Fig. 2). The low-reflectivity areas coincide in places with sedimented bathymetric highs, representing low-relief ridges separated by slightly incised chutes (Figs. 1, 9). The dimensions, frequency and relief of the ridges increase downslope.

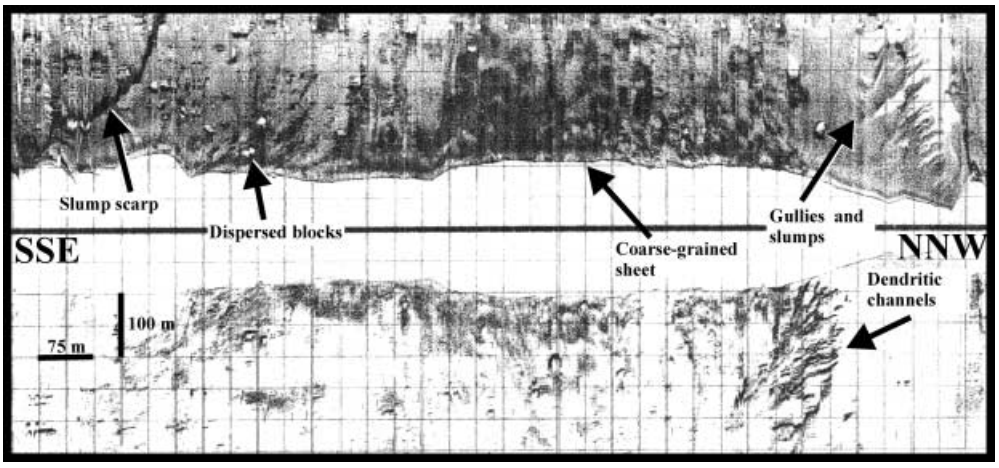

Fig. 6 High-resolution, sidescan sonar line (location in Fig. 1) imaging the upper portion of the Baia di Levante valley from a depth of approximately 480 m (upper limit of figure) to a depth of 550 m (lower limit of figure). Note dendritic channels, gullies and slumps along the northern boundary of the BLV. The central BLV portion has a homogeneous high backscatter texture; dispersed blocks ten of metres across are, however, evident. The scarp which bounds the BLV to the south could be the result of mass-wasting processes. The geometry of along-slope acquisition accounts for the poorer-quality data in the downslope-looking sidescan sonar swath (lower half of the figure)

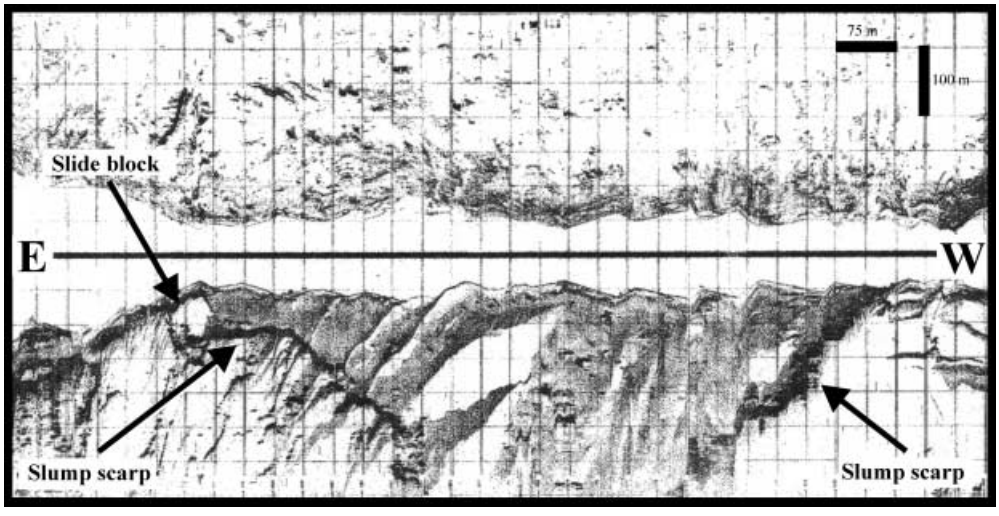

Fig. 7 High-resolution, sidescan sonar image of the southern portion of the upper Baia di Levante valley. The scarp which marks the boundary of the BLV could be the result of mass-wasting processes acting on the slope, as also suggested by the detached slide block adjacent to this feature. The geometry of acquisition accounts for the poorer-quality data in the downslope-looking sidescan sonar swath (upper half of the figure)

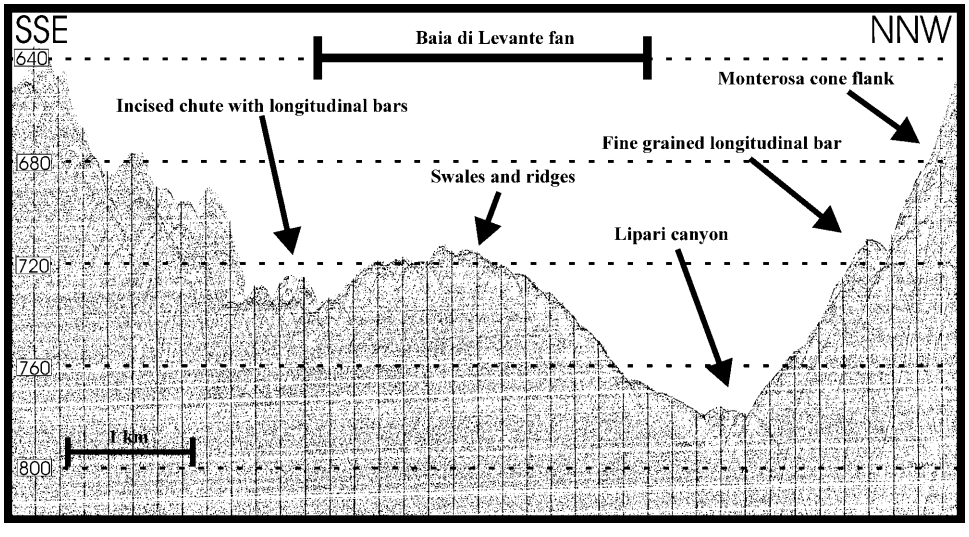

Fig. 8 A 3.5-kHz sub-bottom profile over the Baia di Levante volcaniclastic fan (vertical scale in metres). The surface of the fan is scoured by swales between slightly elevated ridges. The swales and ridges have a very subdued relief and they are not evident on the bathymetric map (Fig. 1). The Lipari canyon is present in the NNW corner of the line. A longitudinal bar with fine-grained sediments is evident between its northern and southern coarse-grained branches

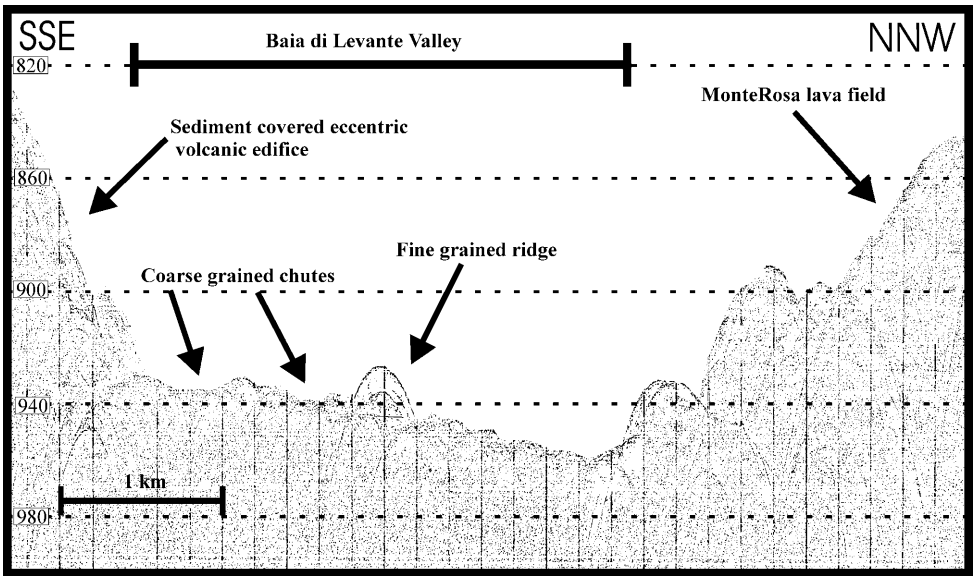

Fig. 9 A 3.5-kHz sub-bottom profile over the lower portion of the Baia di Levante valley incised by chutes cutting through sediment-covered ridges. Note the large ridge in the central portion of the BLV. This is also present in bathymetric map (Fig. 1). The eccentric volcanic edifice to the south of the BLV has a sediment cover up to 15 m thick. The vertical scale is in metres

Discussion

The seafloor features offshore from Vulcano and Lipari have been interpreted in terms of their volcanic and sedimentary processes. The identification of primary volcanic features and of possible clast-forming, transport and depositional processes has allowed the distinction among primary volcanic, resedimented volcaniclastic and volcanogenic sedimentary facies. This facies subdivision follows the genetic classification of volcanic facies used by McPhie et al. (1993) and McPhie (1995), wherein: primary volcanic facies are generated directly and exclusively by volcanic processes; resedimented volcaniclastic facies are composed of clasts initially formed by volcanic processes but then redeposited more or less synchronously with or following directly after eruption with negligible reworking; and volcanogenic sedimentary facies are volcaniclastic deposits that mainly reflect sedimentary processes of transportation and deposition. The resultant facies associations for the Vulcano and Lipari volcaniclastic apron are presented in Fig. 10.

Primary volcanic facies comprise: the submarine portions of the silicic Capo Rosso and Punta Papesca 1 and 2 lavas; the Monterosa submarine cone consisting of pyroclastic deposits covered by coarse-grained volcanogenic sediment; and the Vulcanello offshore seamounts consisting of basaltic pillow lava cones. A submarine volcanic centre is also present south of the BLV, overlain by as much as 15 m of fine-grained sediments indicating that it is not a recent feature.

Reflectivity data reveal some small-scale features of the primary volcanic facies. In particular, the ridges on the surface of the Punta Papesca 1 lava can be interpreted as ogives. In subaerial silicic lavas, ogives have been interpreted either as folds on the surface of the lava (Loney 1968; Fink 1980) or as ramp structures (MacDonald 1972). Surface folds can form only while the lava flow surface remains hot and ductile (Cas and Wright 1987). In the case of the Punta Papesca 1 lava, rapid cooling of the surface in contact with the seawater must have occurred. We therefore interpret the ogives on the surface of this submarine lava as the result of fracturing and ramping of the cool and brittle lava carapace compressed behind the stagnant flow front.

Coarse-grained deposits marginal to and closely associated with the primary volcanic facies have been inferred from the reflectivity data and interpreted as resedimented volcaniclastic facies. Autobrecciation, quench-fragmentation and/or local explosive activity (cf. Cas et al. 1990) would have accompanied the submarine emplacement of the Punta Papesca 1 lava generating voluminous clastic debris. The coarse-grained talus which extends over 1 km^2 as far as 700 m downslope of the lava front (Figs. 2, 10) probably consists of resedimented autoclastic facies derived from the lava. This facies association closely matches that of ancient submarine silicic lavas presently outcropping on land, where coherent lava facies are surrounded by in situ hyaloclastite and distal resedimented facies (Kano et al. 1991; Cas 1992; McPhie and Allen 1992; McPhie et al. 1993).

Coarse-grained talus downslope from the recent volcanic seamounts offshore from Vulcanello is made up of decimetric blocks derived from gravity-driven collapse of unstable lava pillows, resulting in the deposition of pillow-fragment breccia. Sandy deposits marked by high backscatter predominate further downslope and are more difficult to explain. This facies is confined between two bathymetric highs consisting of sediment-covered primary volcanic elements, suggesting that it could comprise deposits of gravity flows, such as turbidity currents or debris flows. We can therefore interpret these deposits as resedimented volcaniclastic debris which could be directly related to volcanic eruptions in the adjoining seamounts, or generated by subsequent gravitational instability.

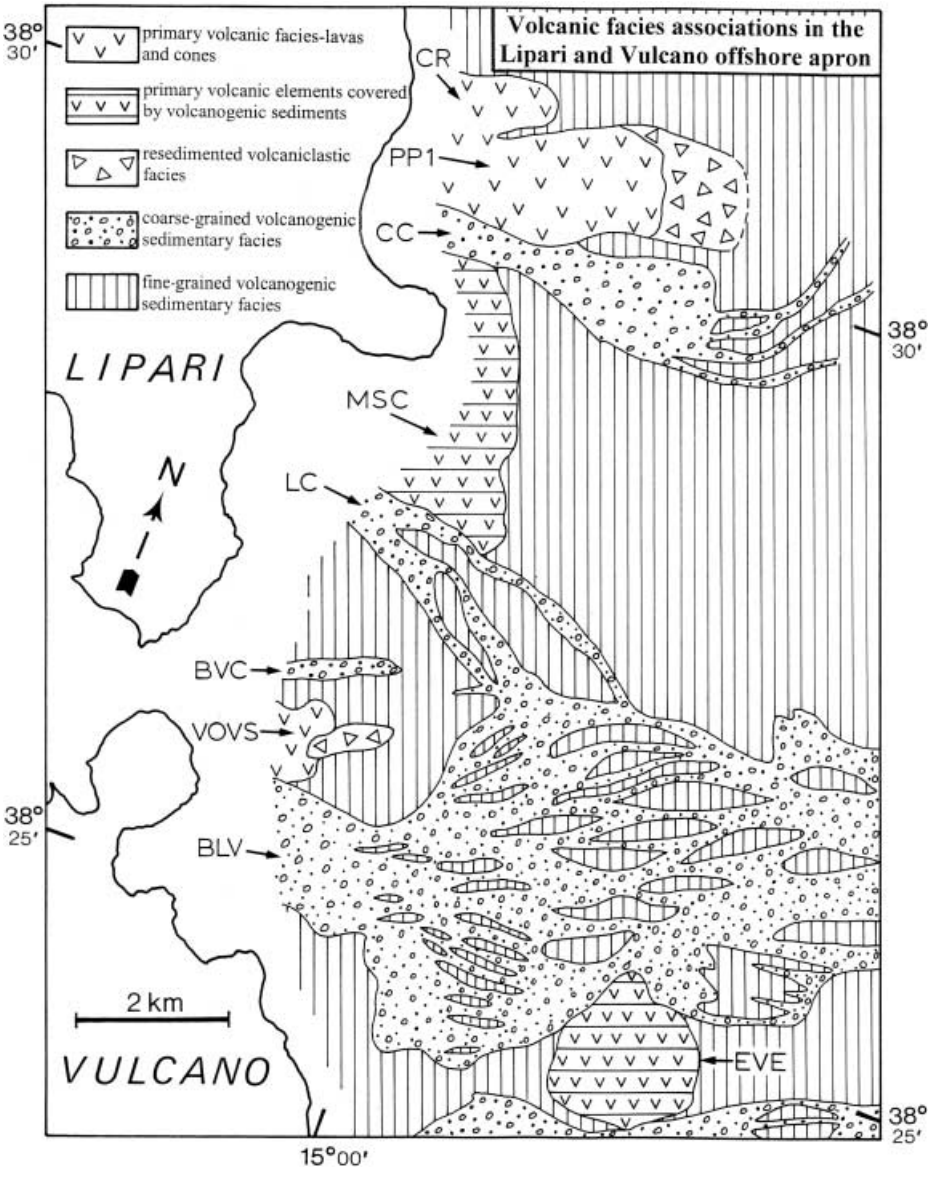

Fig. 10 Present-day facies distribution in the Lipari and Vulcano volcaniclastic apron. Acronyms are the same as in Fig. 1

Volcanogenic sediments, derived mainly from surface weathering, reworking and erosion, are transported to the offshore apron via numerous canyons. Two main canyons dissect the Lipari slope. Their location is controlled by the distribution of submarine primary volcanic elements. The Canneto canyon is confined between the Punta Papesca 1 lava and the Monterosa submarine cone, whereas the Lipari canyon begins at the southern base of the Monterosa submarine cone.

The narrow and steep floor of the Canneto canyon is entirely floored by coarse-grained facies that could be lag deposits from vigorous currents. The 1-km^2 lobe of coarse deposits downslope from the canyon mouth probably developed in response to deceleration of gravity flows because of lateral spreading at the canyon mouth and the observed decrease in gradient. The small (<70 m wide) erosive chutes present downslope suggest that some of the flows bypass this depocentre and continue eroding (Fig. 10).

Coarse-grained facies also occurs on the floor of the uppermost part of Lipari canyon. Here, gravity flows separate downstream, resulting in chutes incised between longitudinal banks on which fine sediment accumulates. Smaller-scale lateral separation of gravity flows is also evident within the Vulcanello canyon.

Gravitational instability on the flanks of La Fossa cone feeds a large volume of coarse-grained material to the offshore apron. The coarse-grained facies on the floor the upper BLV is the result of the prevalence of such mass-wasting processes. Dendritic channels and gullies on the northern side of the BLV reflect the dominance of erosion. The block streams along the southern margin of the BLV could be debris avalanche deposits generated by landslides which affect the emergent La Fossa cone and enter the sea during catastrophic, high-energy events (Rasa' and Villari 1991). Mass-wasting phenomena might also be responsible for the scarp

which bounds the upper portion of the BLV to the south.

The middle BLV volcaniclastic fan shows a subdued morphology consisting of low-relief swales and flanking ridges. The swales are floored by coarse-grained sediment that grades into finer-grained sediment on the ridges. Reflectivity patterns similar to that of the middle BLV have been observed in the upper part of present-day submarine fan deltas, where coarse gravel and sand occur in low-relief swales adjacent to ridges composed of gravelly sand (Prior and Bornhold 1989, 1990; Soh et al. 1995). The lower portion of the BLV is similar, as far as the downslope limit of data, and consists of incised chutes running between low-relief diamond-shaped ridges. The erosional chutes are covered by coarse-grained sediment, whereas finer-grained sediment caps the ridges. Similar seafloor features have been observed in the middle fan zones of the present-day Bear Creek fan deltas (Prior and Bornhold 1989) and in the area downslope of the Fujikawa fan delta (Soh et al. 1995). Concentration- and density-stratified turbidity currents, with basal parts channelised within the swales and chutes and upper parts spreading over larger areas, may be responsible for the observed morphology and sediment distribution over the middle and lower part of the BLV.

Between 1888 and 1892, multiple breaks of a submarine telegraph cable which crosses the BLV occurred (De Fiore 1916). We hypothesise that these events could be related to high-energy gravity flows running along the BLV, rather than to submarine volcanic eruptions as suggested elsewhere (Gabbianelli et al. 1991; Etiope et al. 2000).

Fine volcanogenic sediments that cover the remaining seafloor probably result from water settling of fallout from explosive subaerial eruptions which are frequent on Lipari and Vulcano Islands and from settling from dilute suspensions accompanying gravity flows running in the main canyons and in the BLV.

Conclusion

The Lipari and Volcano offshore apron is dominated by volcanogenic sedimentary facies, which largely exceeds resedimented volcaniclastic and primary volcanic facies. Primary volcanic elements, scattered offshore from Lipari and Vulcano, show various compositions and emplacement mechanisms. They include silicic lavas erupted from vents on land and basaltic pillow lava seamounts. Submarine primary volcanic features, despite their limited areal occurrence, nevertheless play a major role in controlling the facies architecture in the Lipari and Vulcano offshore apron.

Resedimented volcaniclastic facies are closely associated with some of the primary volcanic facies. The Punta Papesca 1 lava is surrounded by coarse-grained talus and an elongate lobe of talus covers the seafloor downslope from the volcanic seamounts offshore Vulcanello. The lobe is confined between two ridges underlain by primary volcanic facies. In this case, the primary volcanic elements acted as a source of debris and also created topography that governed the route for downslope transport and deposition of resedimented volcaniclastic debris.

The primary volcanic facies offshore from Lipari and Vulcano also control the downslope transport of volcanogenic sediment fed from the islands. Canneto and Lipari canyons are walled by primary volcanic elements. Confined gravity flows spread at the base of the flanking volcanic elements, triggering deposition of coarse-grained sediment at the mouth of the Canneto canyon.

Control of the offshore sedimentary evolution by the dynamics of the emergent portions of the volcanic edifices is particularly evident in the area facing Baia di Levante. Here, high-seismicity, ground deformation associated with volcano dynamics, and hydrothermal alteration of the volcanic pile, favour volcano instability resulting in landslides entering the sea. As a consequence, subaqueous gravity flows originating on the upper slope of the BLV generate various depositional and erosional features including a swale-scoured volcaniclastic fan in the middle slope and a chute-incised valley in the lower slope.

Acknowledgements The author is particularly grateful to M. Marani for valuable discussion and assistance during the research and revision of the manuscript in various phases. Thanks go to R. Cas and an anonymous reviewer for the constructive suggestions which improved the paper, and to J. McPhie, responsible editor, for providing helpful comments on the text. The author thanks the Italian Ministry of Industry and G. Patti for granting the use of the data for publication. G. Bortoluzzi, M. Ligi and D. Penitenti are thanked for the processing of the multibeam data. The author gratefully acknowledges L. Masini for technical assistance in the preparation of the figures. G. Zini drafted Fig. 10. This paper is contribution 1257 of the Institute for Marine Geology of Bologna.

References

Achilli V, Baldi P, Baratin L, Bonin C, Ercolani E, Gandolfi S, Anzidei M, Riguzzi F (1998) Digital photogrammetric survey on the Island of Vulcano. Acta Vulcanol 10:1–5

Astis G de, La Volpe L, Peccerillo A, Civetta L (1997) Volcanologic and petrological evolution of Vulcano Island (Aeolian Arc, southern Tyrrhenian Sea). J Geophys Res 102:8021–8050

Barberi F, Innocenti F, Ferrara G, Keller J, Villari L (1974) Evolution of Eolian arc volcanism (southern Tyrrhenian Sea) Earth Planet Sci Lett 21:269–276

Barberi F, Neri G, Valenza M, Villari L (1991) 1987–1990-unrest at Vulcano. Acta Vulcanol 1:95–106

Barberi F, Gandino A, Gioncada A, La Torre P, Sbrana A, Zenucchini C (1994) The deep structure of the Aeolian arc (Filicudi-Panarea-Vulcano sector) in light of gravity, magnetic and volcanological data. J Volcanol Geotherm Res 61:189–206

Cardaci C, Alparone S, Cocina O, Giampiccolo E, Privitera E, Longo V, Velardita S, Biviano A, Marturano M (1988) Vulcano e Stromboli 1. Seismic activity at Vulcano Island and neighbouring area. Acta Vulcanol 10:114–122

Carey S (2000) Volcaniclastic sedimentation around island arcs. In: Sigurdsson H (ed) Encyclopedia of volcanoes. Academic Press, San Diego, pp 627–642

Cas RAF (1992) Submarine volcanism: eruption style, products and relevance to understanding the host-rock successions to volcanic-hosted massive sulfide deposits. Econ Geol 87:511–554

Cas RAF, Wright JV (1987) Volcanic successions, modern and ancient. Chapman and Hall, London, pp 1–528
Cas RAF, Allen RL, Bull SW, Clifford BA, Wright JV (1990) Subaqueous, rhyolitic dome-top cones: a model based on the Devonian Bunga Beds, southeastern Australia and a modern analogue. Bull Volcanol 52:159–174
Crisci GM, Rosa R de, Esperanca S, Mazzuoli R, Sonnino M (1991) Temporal evolution of a three component system: the Island of Lipari (Aeolian arc, southern Italy). Bull Volcanol 53:207–221
Etiope G, Italiano F, Fuda JL, Favali P, Frugoni F, Calcara M, Smriglio G, Gamberi F, Marani M (2000) Deep submarine gas vents in the Aeolian offshore. Phys Chem Earth 25:25–28
Fabbri A, Gallignai P, Zitellini N (1981) Geological evolution of the Peri-Tyrrhenian sedimentary basins. In: Wezel FC (ed) Sedimentary basins of the Mediterranean margins. Tecnoprint, Bologna, pp 101–126
Falsaperla S, Neri G (1986) Contributi sismologici alla sorveglianza vulcanica di Vulcano. Boll GNV 2:243–254
Fink JH (1980) Surface folding and viscosity of rhyolite flows. Geology 8:250–254
Fiore O de (1916) I fenomeni avvenuti a Vulcano (Isole Eolie) dal 1980 al 1913. Zeist Vulkanol 2:12–66
Fisher RV, Schmincke HU (1994) Volcaniclastic sediment transport and deposition. In: Pye K (ed) Sediment transport and depositional processes. Blackwell, Oxford, pp 351–388
Frazzetta G, La Volpe L, Sheridan MF (1983) Evolution of the Fossa Cone. J Volcanol Geotherm Res 17:329–360
Gabbianelli G, Romagnoli C, Rossi PL, Calanchi N, Lucchini F (1991) Submarine morphology and tectonics of Vulcano (Aeolian islands, south-eastern Tyrrhenian sea). Acta Vulcanol 1: 135–141
Gamberi F, Marani MP (1997) Detailed bathymetric mapping of the eastern offshore slope of Lipari island (Tyrrhenian sea): insight into the dark side of an arc volcano. Mar Geophys Res 19:363–377
Gamberi F, Marani MP, Savelli C (1997) Tectonic, volcanic and hydrothermal features of a submarine portion of the Aeolian arc (Tyrrhenian sea). Mar Geol 140:167–181
Gamberi F, Savelli C, Marani MP, Ligi L, Bortoluzzi G, Landuzzi V, Luppi A, Costa M (1998) Contesto morfolotettonico e depositi idrotermali di solfuri ed ossidi di ferro in una porzione sommersa dell'arco eoliano (in base ad indagini ad alta definizione). Boll Soc Geol Ital 117:55–71
Kano KI (1991) Interactions between andesitic magma and poorly consolidated sediments: examples in the Neogene Shirahama Group, south Izu, Japan. J Volcanol Geotherm Res 37:59–75
Loney RA (1968) Flow structure and composition of the southern Coulee, Mono Craters, California: a pumiceous rhyolite flow. Geol Soc Am Mem 116:153–210
MacDonald GA (1972) Volcanoes. Prentice-Hall, Englewood Cliffs, New Jersey, pp 1–375
McPhie J (1995) A Pliocene shoaling basaltic seamount: Ba volcanic group at Rakiraki, Fiji. J Volcanol Geotherm Res 64:193–210
McPhie J, Allen RL (1992) Facies architecture of mineralized submarine volcanic sequences: Cambrian Mount Read volcanics, western Tasmania. Econ Geol 87:587–596
McPhie J, Doyle M, Allen R (1993) Volcanic textures. CODES, University of Tasmania, Hobart, Australia, pp 1–197
Mercalli G, Silvestri O (1891) Le eruzioni dell'isola di Vulcano, incominciate il 3 agosto 1988 e terminate il 22 Marzo 1890. Relazione scientifica. Ann Uff Centr Meteor Geodin 10:1–213
Orton GJ (1996) Volcanic environments. In: Reading HG (ed) Sedimentary environments. Blackwell, Oxford, pp 485–567
Pichler H (1980) The Island of Lipari. Rend Soc Ital Mineral Petrol 36:415–440
Prior DP, Bornhold BD (1989) Submarine sedimentation on a developing Holocene fan delta. Sedimentology 36:1053–1076
Prior DP, Bornhold BD (1990) The underwater development of Holocene fan deltas. In: Colella A, Prior DB (eds) Coarse grained deltas. Int Assoc Sediment Spec Publ 10:75–90
Rasa' R, Villari L (1991) Geomorphological and morpho-structural investigations on the Fossa Cone (Vulcano, Aeolian Islands): a first outline. Acta Vulcanol 1:127–133
Rosa R de, Gillot P, Lanzafame G, Mazzuoli R (1985) The Island of Lipari, IAVCEI Scientific Asembly Excursion Guidebook, Giardini Naxos, Catania Italy 16–21 September, 1985, pp 14–124
Soh W, Tanaka TT, Taira A (1995) Geomorphology and sedimentary processes of a modern slope-type fan delta (Fujikawa fan delta), Suruga Trough, Japan. Sediment Geol 98:79–95
Tinti S, Bortolucci E, Armigliato A (1999) Numerical simulation of the landslide induced tsunami of 1988 on Vulcano island, Italy. Bull Volcanol 61:121–137
Ventura G (1994) Tectonics, structural evolution and caldera formation on Vulcano Island (Aeolian Archipelago, southern Tyrrhenian sea). J Volcanol Geotherm Res 60:207–224
Wright IC (1996) Volcaniclastic processes on modern submarine arc stratovolcanoes: sidescan and photographic evidence from Rumble IV and V volcanoes, southern Kermadec Arc (SW Pacific). Mar Geol 136:21–39